High Strain Rate Compression Behavior of Conventional and CNF-Filled-Nanophased Glass/Polyester Composites

M. K. Hossain*, M. E. Hossain**, M. Hosur*** and S. Jeelani****

*Assistant Professor, hossainm@tuskegee.edu
**Graduate Student, Muhammad.Hossain@tuskegee.edu
***Associate Professor, hosur@tuskegee.edu
****Professor of ME, Director of T-CAM & Ph. D Program in Materials Science and Engineering, and Vice President for Research and Sponsored Program at Tuskegee University, jeelanis@tuskegee.edu
Center for Advanced Materials (T-CAM), Tuskegee University
101 Chappie James Center, Tuskegee, AL 36088, USA

ABSTRACT

The engineering materials are subjected to high strain rate loading in different structural applications and it is deemed necessary to characterize these materials under this loading situations. In this study, a high intensity ultrasonic liquid processor was used to infuse carbon nanofibers (CNFs) into polyester matrix that was then mixed with hardener using a high speed mechanical agitator. The trapped air and reaction volatiles were removed from the mixture using a high vacuum. The conventional and CNFs filled glass/polyester composite laminates using 35 plies of woven E-glass were processed with vacuum assistant resin transfer molding (VARTM). Quasi-static compression tests performed on the unfilled, 0.1 wt. %, 0.2 wt. %, and 0.3 wt% CNF filled Glass/polyester composites, respectively, showed increase in modulus and strength with increasing loading percentage of CNFs up to 0.2 wt%. The better dispersion of 0.2 wt% of CNFs into polyester matrix was observed by scanning electron microscopy (SEM). The high strain rate compressive behavior of this new material system was studied using a Split Hopkinson Pressure Bar (SHPB) setup at strain rates of 550, 700, and 800 s^{-1}. Results showed that the dynamic mechanical strength for both conventional and nanophased glass reinforced polyester increases with increasing strain rates. Fracture morphology of compression tested specimens examined under scanning electron microscope (SEM) revealed fiber kinking and shear fracture at low strain rates, with global delamination, interfacial separation, matrix cracking, fiber breakage and matrix-fiber debonding dominating at high strain rate failure regime.

Keywords: Polyester, CNFs, VARTM, Split Hopkinson Pressure Bar, High Strain Rate.

1 INTRODUCTION

Fiber reinforced polymer matrix composites (FRPC) have become attractive structural materials in aerospace industry, marine, armor, automobile, railways, civil engineering structures, sport goods [1] due to their high specific strength and specific stiffness to weight ratios, fatigue properties, and corrosion resistance. Depending on the service conditions, many of these structures are prone to dynamic loadings such as high impact loads. Hence, it is necessary to have a good knowledge on the high strain rate compression behavior of polymer composites reinforced with nanoparticles, such as carbon nanptubes (CNT), carbon nanofibers (CNF), clay nanoplatelets, and other nanoparticles. Hayes et al. [2] have shown the ability to incorporate nanosized alumina structures in the matrix and interlayer regions of prepreg based carbon/epoxy composites.

Ochola et al. [3] studied the strain rate sensitivity of both carbon fiber reinforced polymer (CFRP) and glass fiber reinforced polymer (GFRP) at strain rates of 10^{-3} and 450 s^{-1}. They documented the dynamic strength for GFRP increases with increasing strain rates and the strain to failure for both composites decrease with increasing strain rates. Evora and Shukla [4] investigated the dynamic response of polyester/TiO_2 nanocomposites under high strain rate (2000 s^{-1}) compression loading and obtained results showed that the addition of nanoparticles contributed to a moderate stiffening effect, but there was no significant effect on ultimate strength. Guo and Li [5] also concluded the compressive strength of SiO_2 filled epoxy nanocomposites was higher than that of pure epoxy at the high strain rate. Montiel and Williams [6] reported the dynamic behavior of AS4 graphite/PEEK cross-plied composites laminates at strain rate upto 8 s^{-1} using a drop tower assembly and documented 42 and 25% increased in strength and strain to failure, respectively, over the static values. Hosur et al. [7] studied the high strain compression response of affordable woven carbon/epoxy composites and found considerable increase in dynamic compression peak stress as compared to static loading; whereas the strain at peak stress was lower by 35–65%. Guden et al. [8] found the modulus and failure strength of woven glass fiber/ SC-15 composites to be strain rate sensitive and the failure of the composite occurred through matrix fracture and delamination.

In this study, glass/polyester nano-composites with 0.1wt.%, 0.2 wt.% and 0.3 wt.% CNFs loading and conventional ones were fabricated. Quasi-static compression tests showed the improvement in properties of nanophased composites compare to the conventional ones. Both conventional and nanophased composites were characterized using Split Hopkinson Pressure Bar (SHPB) setup and fracture morphology was examined using SEM. The experimental results of the new material system obtained were used to assess the influence of CNF on the properties of glass/polyester nanocomposites.

2 EXPERIMENTAL

2.1 Materials Selection

Commercially available B-440 premium polyester resin and styrene from US Composite, heat treated PR-24 CNF from Pyrograf Inc., and woven E-glass fiber from fiberglasssite.com were considered as matrix, nanoparticle, and reinforcement, respectively, in this current study because of their good property values and low cost. Polyester resin contains two-part: part-A (polyester resin) and accelerator part-B (MEKP- methyl ethyl ketone peroxide).

2.2 Resin Preparation

Ultrasonic cavitation technique is one of the most efficient means to disperse nanoparticles into a polymer [9]. In this study, sonication was performed using a high intensity ultrasonic irradiation (Ti-horn, 20 kHz Sonics Vibra Cell, Sonics Mandmaterials, Inc, USA) for 90 minutes, adding 0.1, 0.2, and 0.3wt.% CNF with corresponding percent polyester resin with 10 wt% styrene in a glass beaker. To remove the bubbles, high vacuum was applied using Brand Tech Vacuum system for about 90-120 minutes. Once the bubbles were completely removed from the mixer, 0.7 wt% catalyst was mixed with the mixer using a high-speed mechanical stirrer.

2.3 Composite Fabrication

Both conventional and nanophased E-glass/CNF-polyester composites were manufactured by VARTM process. The panel was cured for about 12-15 hours at room temperature. The room temperature cured material was taken out from the vacuum bagging and trimmed, and test samples were machined according to ASTM standard. They were thermally post cured at 110 °C for 3 hours in a mechanical convection oven.

2.4 Test Procedure

Quasi-static tests were performed on the servo-hydraulic MTS testing unit according to ASTM D695 to determine the ultimate strength and young modulus of the glass/polyester composites. The machines were run under the displacement control mode at a crosshead speed of 1.27 mm/min and tests were performed at room temperature.

For high strain rate testing, a modified SHPB test setup was used in this study. Typical setup of modified SHPB is shown schematically in Figure 1. Details of the setup and stress reversal technique are discussed by Hosur et al. [10]. During high strain rate loading, specimen is sandwiched between the incident bar and the transmission bar. Petroleum jelly is applied at surfaces of the specimen in contact with the bars to reduce the effect of friction.

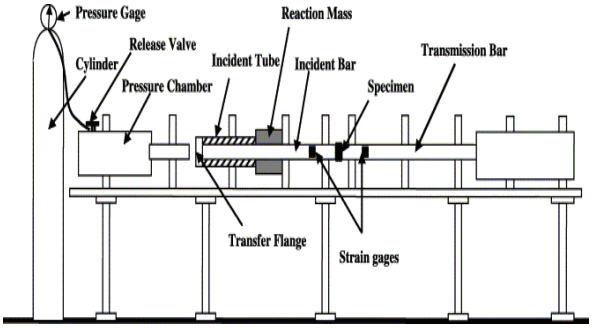

Figure 1: Schematic of compression Split Hopkinson Pressure Bar setup

The transient strain history was recorded from the strain gages mounted on the incident and the transmission bars. Two gages were mounted diametrically opposite to each other on each bar to eliminate recording of any bending strains. The data was acquired using a high-speed data acquisition card with Gagescope V3.42 software at a sampling rate of 2 MHz. The stress–strain relation was developed based on one dimensional elastic bar-wave theory for a pulse propagating in a uniform bar, which was initially unstrained and at rest before the pulse arrives. For this data analysis, VuPoint signal analysis software was used.

Fractography of neat and nanocomposite samples was studied using a Field Emission Scanning Electron Microscope (FE-SEM Hitachi S-900) JEOL JSM 5800). An accelerating voltage was applied to accomplish desired magnification. Fracture morphology of quasi-static tested samples was examined using SEM.

3 RESULTS AND DISCUSSIONS

3.1 Quasi-static Tests

Quasi-static tests were performed on the Neat, 0.1, 0.2, and 0.3 wt.% CNF-filled glass reinforced polyester nanocomposites (CNF-GRPC) to evaluate their compression stiffness and strength. Their typical stress-strain behaviors are shown in Figure 2. It is clear from these

stress-strain curves that all the samples of CNF-filled nanophased E-glass/polyester composites showing considerable nonlinearity before reaching the maximum stress. However, more or less ductility was observed in each type of laminate sample but no obvious yield point was found.

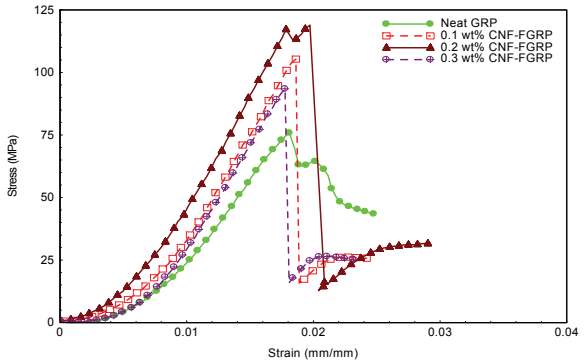

Figure 2: Stress-strain curves of GRPC and CNF-GRPC

Five samples were tested for each condition and the average properties obtained from these tests. It is evident that for 0.2 wt.% CNF loaded GRPC the compressive strength and modulus increased by about 43 and 71%, respectively, as compared to the neat GRPC samples. Quasi-static compression results are given in Table 1.

GRP and wt% CNF-FGRP	**Max. Stress (MPa)**	**% Change**	**Modulus (GPA)**	**% Change**
Neat	80.72 ± 6.27	------	3.78 ± 0.25	------
0.1wt%	106.98 ± 1.65	32.50	5.52 ± 0.48	46.03
0.2wt%	**115.71 ± 3.25**	**43.35**	**6.45 ± 0.27**	**70.64**
0.3wt%	95.4 ± 2.75	18.19	5.14 ± 0.44	35.98

Table 1: Quasi-static results of GRPC and CNF-GRPC

3.2 High Strain Rate Tests

The High strain rate tests were performed on 35 ply GRPC and CNF-GRPC at three different strain rates of 550, 700 and 800 s^{-1}, respectively. The transient data for each sample tested under high strain rate data was recorded and stored. The data is triggered at the point when the initial compressive pulse reaches the location of the strain gage on the incident bar. The strain rate versus time and stress versus time data are stored in separate files. To plot the dynamic stress–strain curve, it is important to synchronize the two pulses. The starting time is selected from the transmitted pulse at the instant when it starts deviating from zero and the ending time is selected as the time when the transmitted pulse flattens out. The portion of the reflected pulse is chosen for the corresponding time range and integrated to get the strain versus time data. Strain versus time and stress versus time data are superimposed by choosing stress for the *y*-axis and strain for the *x*-axis to obtain stress–strain curve. The data for dynamic tests is summarized in Table 2, which gives the peak stress, the slope of stress–strain curves, and the average values. To determine the modulus (slope of stress–strain curve), linear portion of the curve is zoomed in using Easyplot graphic software. The zoomed in portion is then fitted with a linear curve. Slope of the linear fit equation gives the stiffness of the sample. Figures 3 and 4 illustrated dynamic stress-strain curves of conventional and nanophased GRPC at different strain rates at room temperature.

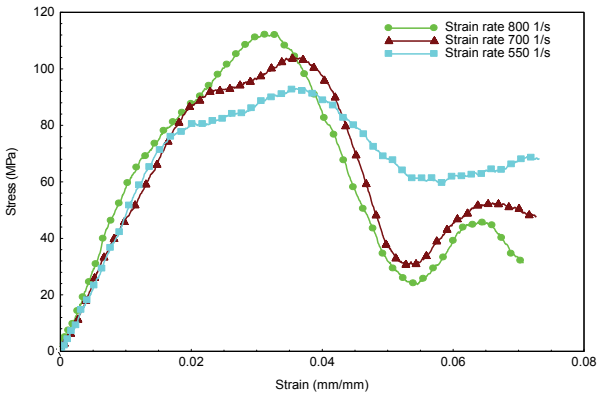

Figure 3: Typical stress –strain curve for neat GRPC

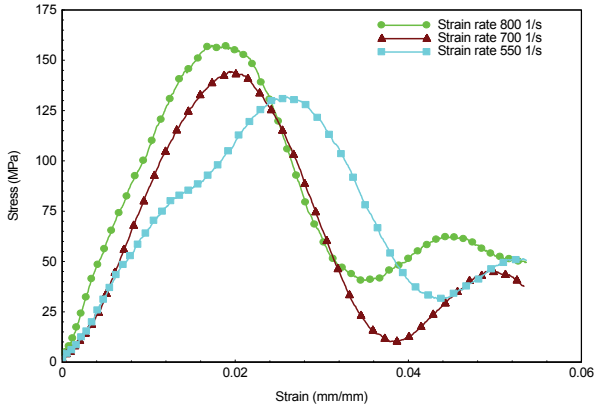

Figure 4: Stress-strain curve for 0.2 wt.% CNF-GRPC

The average modulus in both conventional and nanophased composites increases as the strain rate increases from quasi-static to high strain rates. The average maximum stress within the strain rate regimes also increases with increasing strain rate from quasi-static value to high strain rates. But the strain at failure slightly decreases with increasing strain rates and addition of CNFs.

Composites	Strain rates, 1/s	550	700	800
Neat GRPC	Max. Stress, MPa	92	103	110
	Modulus, GPa	4.87	4.93	5.05
0.2 wt.% CNF -GRPC	Max. Stress, MPa	126	140	152
	Modulus, GPa	7.01	8.85	10

Table 2: Summarized results from dynamic tests

Also at higher strain rates (550, 700, 800 s^{-1}), both the failure stress and modulus increases nonlinearly with increasing strain rates in both conventional and nanophased GRPC. The strain rate sensitivity on failure stress showed in Figure 5.

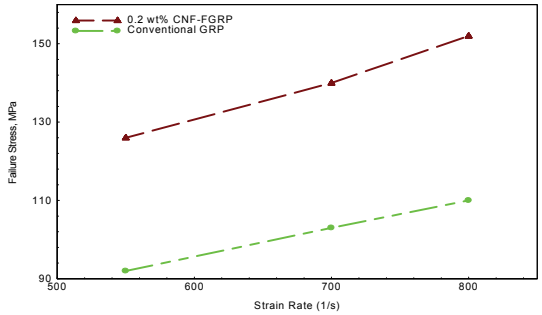

Figure 5: Failure stress vs. strain rate of GRPC

3.3 Fracture Morphology

Fracture morphology of quasi-static tested samples was studied using SEM. The SEM micrographs of the fractured surfaces of GRPC and CNF-GRPC are illustrated in Figures 6 and 7. Comparative analyses of the fractured surfaces of GRPC and CNF-GRPC showed that the CNF-GRPC exhibited less region of the fiber–matrix separation, matrix breaking due to better addition in presence of CNFs and the conventional GRPC showed huge region of fiber-matrix debonding, matrix breaking, fiber breaking, and spalling of the matrix.

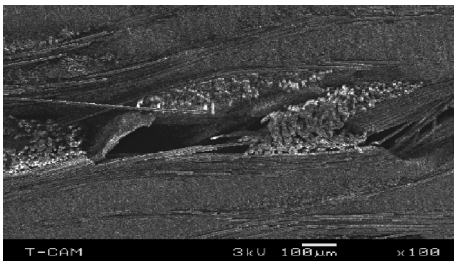

Figure 6: Fracture of 0.2% CNF-GRPC

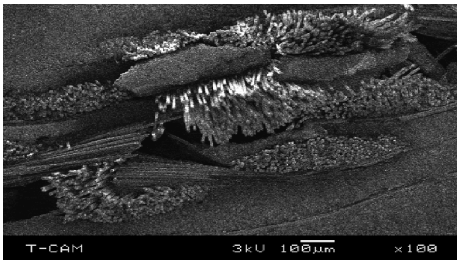

Figure 7: Fracture of conventional GRPC

4 CONCLUSIONS

Compression responses of plain weave GRPC and GRP-CNF-GRPC were carried out at high strain rates. The significant conclusions drawn from the investigation are given below.

1. 0.2% CNF-GRPC exhibited the 43 and 71% improvement of compression strength and flexural modulus, respectively.
2. High strain rate test also illustrated that dynamic responses of laminate showed a strong influence of CNFs addition with the GRPC. In both the cases, there was also a considerable increase in the peak stress and stiffness at high strain rate loading as compared to lower strain rate loading.
3. Both failure stress and modulus increased nonlinearly with increasing strain rates in both conventional and nanophased GRPC.
4. SEM studies revealed the better adhesion of fiber – matrix in the CNF-GRPC due to the uniform dispersion of the CNFs and showed less damage.

REFERENCES

[1] Millerschin, E., Compos. Fab., 40-42, 1999.
[2] Hayes, B. S., Nobelen, M., Dharia, A. K. and Seferis J. C., 33rd International SAMPE Symposium and Exhibition, Seattle, WA, 2001.
[3] Ochola, R.O., Marcus, K., Nurick, G. N. and Franz, T., Compos. Struct., 63, 455-467, 2004.
[4] Evora, V., M. F., and Shukla, A., Mat. Sci. and Eng. A, 361, 358-366, 2003
[5] Guo, Y. and Li, Y., Mater. Sci. and Eng. A, 458, 330-335, 2007.
[6] Monteal, D. M. and Williams, C. J., ASTM STP 1120(10), 54–65, 1992.
[7] Hosur, M.V., Alexander, J., Jeelani, S., Vaidya, U.K. and Mayer, A. , J. Reinf. Plast. Compos, 22(3), 271–296, 2003.
[8] Guden, M., Yildirim, U. and Hall, I. W., Polymer Testing, 23, 719-725, 2004
[9] Eskin, G.I., Ultrasonic Sonochemistry, 8 (3), 319-325, 2001.
[10] Hosur, M. V., Alexander, J., Vaidya, U.K. and Jeelani, S., Compos. Struct. 52, 405–417, 2001.